JACS
JOURNAL OF THE AMERICAN CHEMICAL SOCIETY
Article
Cite This: J. Am. Chem. Soc. 2019, 141, 1583−1592
pubs.acs.org/JACS

A Hendecad Motif Is Preferred for Heterochiral Coiled-Coil Formation

Dale F. Kreitler,[†,#] Zhihui Yao,[‡] Jay D. Steinkruger,[§] David E. Mortenson,[†,▽] Lijun Huang,[∥] Ritesh Mittal,[∥] Benjamin R. Travis,[∥] Katrina T. Forest,*[,†,‡,⊥] and Samuel H. Gellman*[,†,‡]

[†]Department of Chemistry, University of Wisconsin—Madison, Madison, Wisconsin 53706, United States
[‡]Graduate Program in Biophysics, University of Wisconsin—Madison, Madison, Wisconsin 53706, United States
[§]School of Natural Sciences, University of Central Missouri, Warrensburg, Missouri 64093, United States
[∥]Anatrace, Maumee, Ohio 43537, United States
[⊥]Department of Bacteriology, University of Wisconsin—Madison, Madison, Wisconsin 53706, United States

Supporting Information

ABSTRACT: The structural principles that govern interactions between L- and D-peptides are not well understood. Among natural proteins, coiled-coil assemblies formed between or among α-helices are the most regular feature of tertiary and quaternary structures. We recently reported the first high-resolution structures for heterochiral coiled-coil dimers, which represent a starting point for understanding associations of L- and D-polypeptides. These structures were an unexpected outcome from crystallization of a racemic peptide corresponding to the transmembrane domain of the influenza A M2 protein (M2-TM). The reported structures raised the possibility that heterochiral coiled-coil dimers prefer an 11-residue (hendecad) sequence repeat, in contrast to the 7-residue (heptad) sequence repeat that is dominant among natural coiled coils. To gain insight on sequence repeat preferences of heterochiral coiled-coils, we have examined three M2-TM variants containing substitutions intended to minimize steric clashes between side chains at the coiled-coil interface. In each of the three new crystal structures, we observed heterochiral coiled-coil associations that closely match a hendecad sequence motif, which strengthens the conclusion that this motif is intrinsic to the pairing of α-helices with opposite handedness. In each case, the presence of a hendecad motif was established by comparing the observed helical frequency to that of an ideal hendecad. This comparison revealed that decreasing the size of the amino acid side chain at positions that project toward the superhelical axis produces tighter packing, as determined by the size of the coiled-coil radius. These results provide a basis for future design of heterochiral coiled-coil pairings.

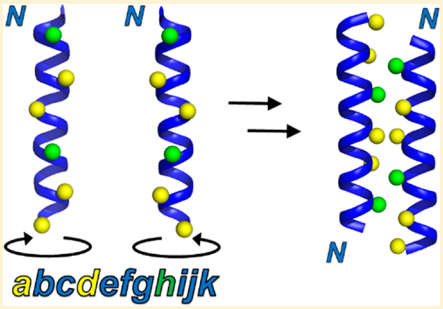

INTRODUCTION

Polypeptides composed exclusively of D-α-amino acid residues are of interest for biomedical applications because they resist degradation by natural proteases, a major shortcoming of peptides composed entirely of L-residues. Potential uses of D-peptides include inhibition of disease-associated protein−protein interactions, which requires D-peptides that engage specific recognition surfaces on L-protein targets.[1−3] Generating D-peptides with the requisite binding properties, however, can be challenging. Mirror-image phage display has facilitated the discovery of D-peptides that interfere with several protein−protein interactions,[1−6] but this method requires chemical synthesis of the enantiomer of the target protein, which limits target protein size. The retro-inverso design strategy has been successful for some antibodies,[7] but this method has failed in other cases.[8] The relatively small number of high-resolution structures showing how D-peptides bind to complementary surfaces on L-proteins has made it difficult to identify structural principles that govern heterochiral associations.[1,2,6]

Coiled coils are assemblies formed by α-helices and are probably the best understood motif in protein tertiary and quaternary structure.[9−11] The simplest examples are dimeric, with either parallel or antiparallel orientation of the α-helical backbones. Coiled-coil interactions play essential roles in membrane fusion, cytoskeletal movement, DNA transcription, and many other biological processes.[9] In canonical coiled coils, hydrophobic residues are found in a heptad repeat pattern, conventionally designated ***abcdefg***, with residues at positions ***a*** and ***d*** typically bearing nonpolar side chains. In an α-helix, this sequence pattern causes the nonpolar side chains to be projected in a stripe along one side of the helix. Coiled-coil association is driven by burial of hydrophobic side chains; efficient packing requires that the helices twist around a central superhelical axis to compensate for the discrepancy in periodicity between a heptad repeat pattern (3.50 residues/turn) and that of an ideal α-helix (3.65 residues/turn).[10,12]

Received: October 18, 2018
Published: January 15, 2019

DOI: 10.1021/jacs.8b11246
J. Am. Chem. Soc. 2019, 141, 1583−1592

These well-established principles were first identified in 1952 by Crick, who subsequently derived a set of parametric equations that accurately describes coiled-coil geometry.[9−15] Recent computational efforts based on iterations of the Crick equations demonstrate that L-α-amino acid sequences can be designed de novo to form coiled-coil assemblies with specific and diverse stoichiometries and geometries.[16−19]

The advanced state of homochiral coiled-coil design suggests that *heterochiral* coiled coils represent an excellent starting point for developing principles that govern interactions between L- and D-peptides. Indeed, Crick laid the groundwork for such an effort by noting that helices of opposite handedness should "mesh together" in a manner akin to two gears of opposite sense, i.e., that the helices in a heterochiral coiled-coil dimer should not manifest the superhelical twist that is characteristic of homochiral coiled-coils due to the opposite sense of enantiomorphic helices.[13] Contemporaneously, Pauling and Corey proposed that heterochiral mixtures of peptides could form "rippled" β-sheets.[20] Crick's prediction is consistent with the first high-resolution heterochiral coiled-coil structures, which were recently determined by our groups.[21] These structures were obtained by crystallizing the racemate of a peptide designated M2-TM, which corresponds to a single helical transmembrane (TM) segment of the influenza A M2 protein.[22]

In an effort to augment understanding of the factors that control heterochiral coiled-coil dimer formation, we have now determined racemate structures for three single-point variants of M2-TM. Collectively, these structures strengthen the conclusion[21] that heterochiral coiled-coils are optimally generated with an 11-residue or hendecad repeat (3,4,4 spacing) of hydrophobic side chains rather than the heptad repeat (3,4 spacing) that is most common among homochiral coiled-coils. The new structures shed light on relationships between interfacial side chain size and heterochiral coiled-coil packing.

RESULTS AND DISCUSSION

Structural Considerations. An ideal, linear α-helix has a periodicity of 3.65 residues/turn[23] (98.6°/residue). Therefore, alternating separations of three and four residues (3,4 spacing) between buried hydrophobic side chains will place the side chains at positions i+3 and i+7 on approximately the same side of an α-helix as the side chain of residue i. This heptad sequence pattern encompasses slightly less than two turns of an ideal α-helix (~690° vs 720°). This small discrepancy results in a drift of the hydrophobic side chain array projected by a linear α-helix relative to the residue register. For a right-handed α-helix, formed by a peptide composed exclusively of L-residues, there is a left-handed drift of the hydrophobic array relative to the helix axis. A left-handed α-helix, formed by a D-peptide, therefore displays a right-handed drift of the hydrophobic array relative to the helix axis (Figure 1).

The helices within a homochiral coiled-coil dimer compensate for the drift in the hydrophobic side chain display, which has the same sense for each partner, by supercoiling around the interhelical axis. Since helices formed from D-peptides display a side chain drift of opposite sense relative to helices formed from L-peptides, supercoiling cannot optimize the packing of extended hydrophobic surfaces in a heterochiral coiled-coil dimer. Thus, the 3,4-spacing pattern (heptad repeat) is not optimal for heterochiral coiled-coil associations beyond approximately four α-helical turns.[24] Extending the

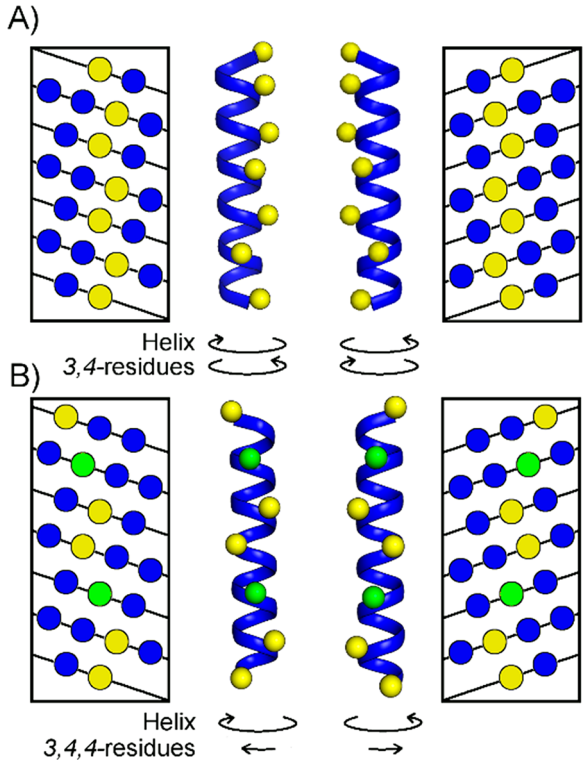

Figure 1. Helical net diagrams map the 3D surface of a helix to a 2D display with periodic boundary conditions based on three- and four-residue repeats (each approximately one turn of the helix). (A) Knob positions are indicated in yellow for a 3,4-spacing pattern (*abcdefg*; yellow for *a* and *d* positions) for a left-handed (left panel) and right-handed (right panel) α-helix. (B) Insertion of a four-residue stutter results in the formation of an *h* position (*abcdefghijk*; *h* position green) that is flanked by two four-residue spacings for a left-handed (left panel) and right-handed (right panel) helix. In both (A) and (B), the helical chirality is compared to the chirality of the hydrophobic interface. The set of arrows directly underneath each helix represent the handedness of the helix. The second set of arrows directly underneath the first set represents the handedness of the hydrophobic interface, and the lengths of these arrows are approximately scaled in length to represent the magnitude of the frequency of hydrophobic residue display for each interface.

3,4-spacing pattern by one helical turn generates a 3,4,4-spacing pattern (11 residue; hendecad repeat) that encompasses slightly more than three turns of an ideal α-helix (1085° vs 1080°). An α-helix with a slightly elevated periodicity of 3.67 residues/turn (98.2°/residue) would align every 11th residue along the helix axis. Because the discrepancy between this value and the 3.65 residues/turn of a linear α-helix is small, the hydrophobic side chain array displayed by a linear α-helix with 3,4,4-spacing approximates a stripe that is parallel to the helix axis, albeit with a tiny right-handed drift[25,26] (Figure 1). Therefore, a 3,4,4-spacing of nonpolar side chains at the sequence level should avoid the need for supercoiling around the interhelical axis and be more amenable to heterochiral coiled-coil assembly than is a 3,4-spacing. Here we use ***abcdefghijk*** to describe positions in the hendecad repeat unit that is consistently manifested in our crystal structures. Nonpolar side chains are found at positions ***a***, ***d***, and ***h***.

The hendecad motif is occasionally observed within naturally occurring coiled-coils and described as a four residue "stutter" insertion.[9,27−29] Perturbations in canonical coiled-coil geometry that arise from stutter insertions have been identified

DOI: 10.1021/jacs.8b11246
J. Am. Chem. Soc. 2019, 141, 1583−1592

previously by Lupas et al.,[9,28] who noted the 11-residue periodicity should create a less tightly wound supercoil upon dimerization than a heptad pattern. In such dimers, the side chain in the hendecad *h* position is shifted into the supercoil axis of the coiled-coil interface relative to a canonical heptad *a* position (*abcdefghijk* vs *abcdefgabcd*). The side chains of residues at hendecad *a* and *d* positions flank a central cavity occupied by side chains from residues situated at the *h* positions. Hendecad motifs have been observed for both parallel and antiparallel homochiral assemblies.[9,28,30] In either the parallel or antiparallel homochiral case, close associations between *h* positions on opposing helices result in knob-to-knob (KTK) interactions that deviate from canonical knob-into-hole (KIH) packing (Figure 2).

Our recent efforts[21] produced two distinct high-resolution structures of the M2-TM racemate, one from a lipidic cubic phase (LCP; PDB: 4RWB) and the other from a solution containing racemic *β*-octylglucoside (OG; PDB: 4RWC). The LCP-derived structure displayed a 3,4,4-spacing pattern. The OG-derived structure featured a geometry similar to that of the LCP structure; however, the helices were offset, and the resultant coiled-coil exhibited a 3,4-spacing pattern over four turns (Figure 3). From this pair of structures, it was unclear whether the hendecad motif evident in the LCP-derived structure was an artifact of crystallization or an inherent feature of heterochiral coiled-coil interfaces. The studies described here were intended to address this uncertainty.

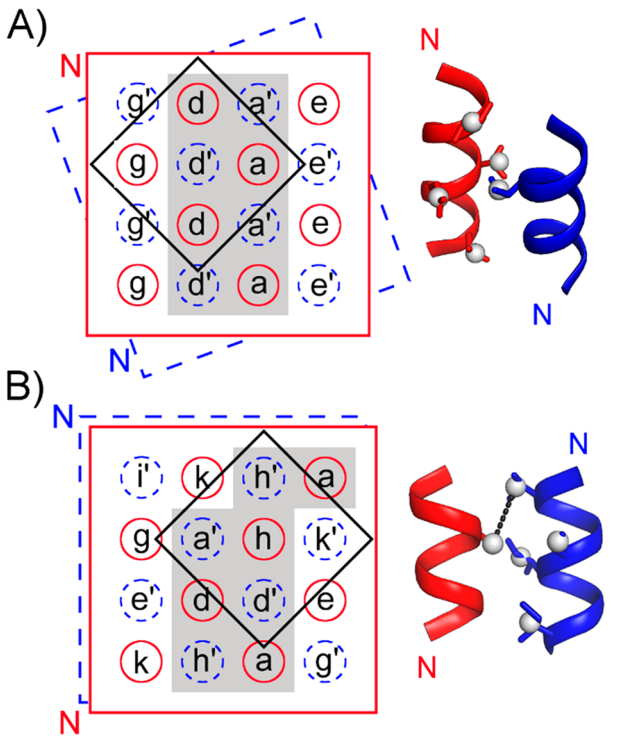

Figure 2. Helical net diagrams and corresponding 3D displays for homochiral and heterochiral antiparallel coiled-coil dimers.[24] Net diagrams are truncated to display only residues at or immediately adjacent to the coiled-coil interface. Opposing helices are represented as solid or dashed lines. Side chain centers of mass are represented as gray spheres. (A) Antiparallel homochiral dimer (PDB 3GPV) with 3,4 spacing (heptad repeat). (B) Antiparallel heterochiral dimer (M2-TM I39A) with 3,4,4 spacing (hendecad repeat). In the helical net images, the residues that serve as knobs are highlighted in gray (*a* and *d* positions for the homochiral dimer; *a*, *d*, and *h* positions for the heterochiral dimer). A representative KIH interaction is indicated with a black diamond in each case. The opposite helical sense of the two peptides precludes supercoiling. Lack of supercoiling disrupts canonical KIH interactions and results in KTK interactions, which involve steric repulsion. The KTK interaction between the *h* position side chains is represented as a black dashed line in the image on the right.

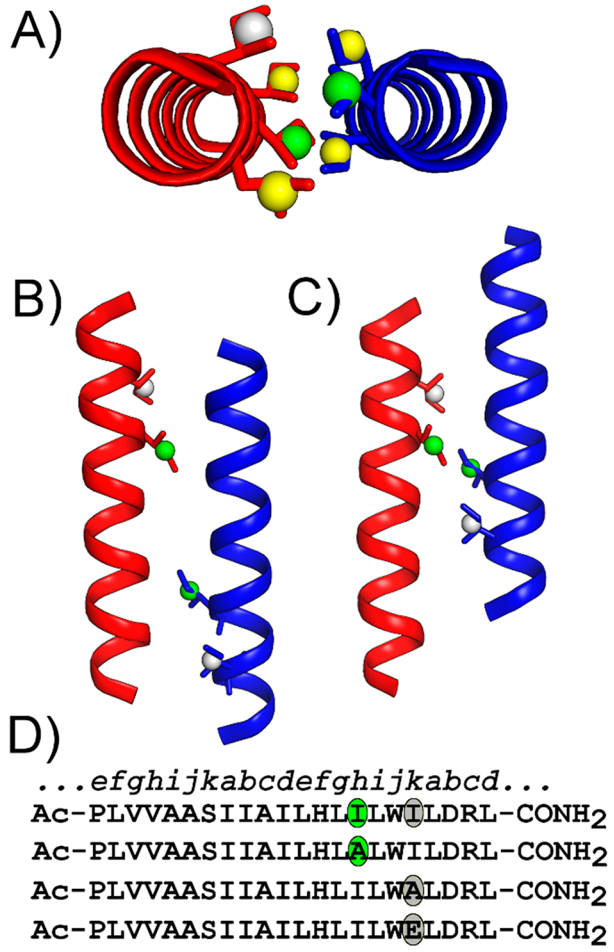

Figure 3. Images from the crystal structures of racemic M2-TM LCP (PDB 4RWB) and M2-TM OG (PDB 4RWC) and sequences of M2-TM and new variants. (A) View along the helix axes of the antiparallel heterochiral coiled-coil dimer in M2-TM LCP (D-helix, red; L-helix, blue); *h* position side chains (green spheres) project into the interface and are flanked by *ad* position side chains (yellow spheres) and *k* position side chain (gray sphere). (B) View perpendicular to (A). The *h* position and *k* position residues that were modified in this study are shown for the view perpendicular to the helix axes for the (B) M2-TM LCP and (C) M2-TM OG dimer. (D) Sequences of M2-TM (top) and variants I39A, I42A, and I42E, with substitution positions indicated in green (hendecad *h* position) and gray (hendecad *k* position), aligned with a hendecad registry.

Selection of Substitution Positions. Homochiral coiled-coil dimer interfaces feature KIH interactions in which side chain knobs from one helix pack into a four-residue hole from the other helix (Figure 2A). Knob and hole identities are interwoven; side chains at the *a* and *d* positions of each helix play both roles, and the identity of residues at these positions can influence homochiral coiled-coil orientation and oligomeric state.[12] To test the hypothesis that a hendecad motif is more favorable than a heptad motif for a heterochiral interface,

DOI: 10.1021/jacs.8b11246
J. Am. Chem. Soc. 2019, 141, 1583−1592

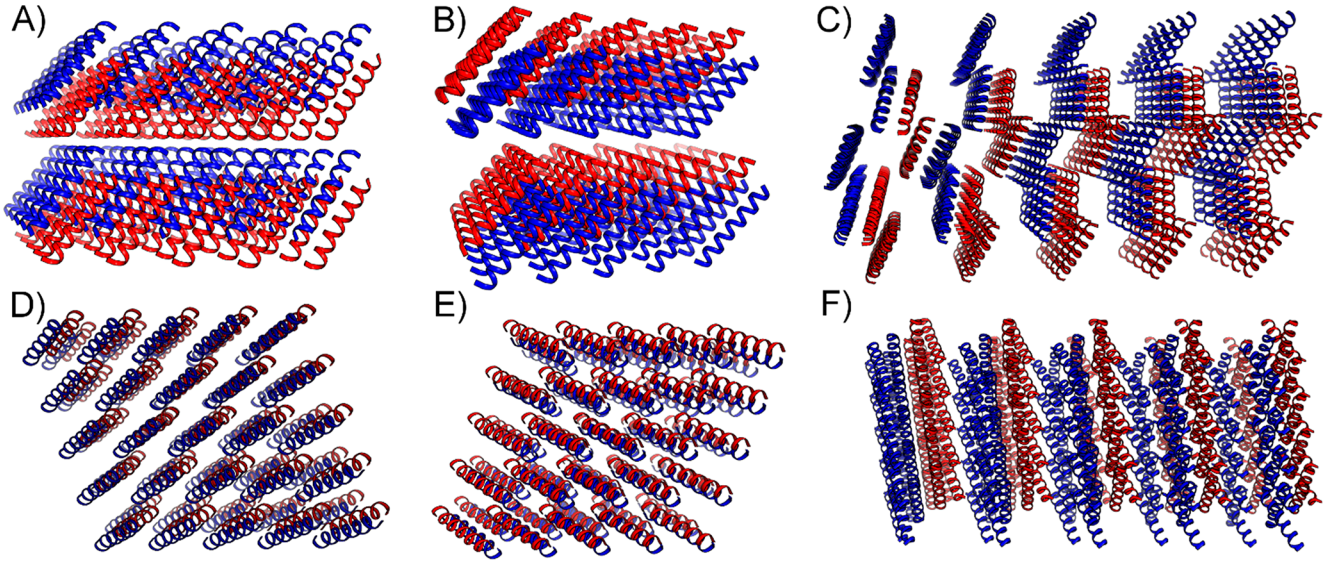

Figure 4. Packing patterns in the three new crystal structures. (A, D) M2-TM I39A (6MPL, type I packing). (B, E) M2-TM I42A (6MPM, type I packing). (C, F) M2-TM I42E (6MPN, type II packing). Each panel displays two unit cells in the *c*-direction and five unit cells in the *a*- and *b*-directions. Unit cells are oriented so that the *ab*-plane is (A−C) perpendicular or (D−F) parallel with the plane of the page.

amino acid substitutions of either Ile → Ala or Ile → Glu were evaluated at M2-TM positions Ile39 (heptad, knob/hole; hendecad, knob/hole) and Ile42 (heptad, knob/hole; hendecad, hole; Figure 3). The small, hydrophobic side chain of alanine can be accommodated within both motifs, whereas the larger, charged side chain of glutamate would be more suitable in the hendecad motif at a hole position.

Crystallization of New Racemates. Racemic crystallization of M2-TM variants I39A (PDB: 6MPL), I42A (PDB: 6MPM), and I42E (PDB: 6MPN) afforded crystals that led to X-ray crystal structures of 1.55, 1.40, and 1.40 Å resolution, respectively. Efforts to obtain crystals for M2-TM I39E were unsuccessful. In each case, the M2-TM racemate was crystallized from an aqueous solution of racemic *β*-octyl-glucoside (2% w/v) using hanging drop vapor diffusion (for details regarding peptide synthesis, purification, and crystallization procedures, see the Supporting Information). Each racemic M2-TM variant crystallized in space group *P*-1. All three structures contain antiparallel heterochiral dimeric coiled coils, in which individual helices within a dimer are related by a crystallographic inversion center. M2-TM I39A and I42A both contain one L- and one D-peptide in the unit cell, and both display type I crystal packing.[31] These structures feature a lamellar assembly of hydrophobic peptide layers, an arrangement commonly observed in membrane protein crystals that are grown from lipid mesophases.[31,32] In the M2-TM I39A and I42A structures, lamellae comprise heterochiral dimers that are aligned at a slightly acute angle relative to the normal vector of the lamellae (Figure 4).

The M2-TM I42E structure contains two L-peptides in the asymmetric unit and, thus, two unique heterochiral interfaces. This structure displays type II crystal packing, a packing mode commonly observed in crystals of soluble proteins. Type II crystal packing is manifested as a 3D lattice pinned together by polar contacts between polypeptides.[31] Among membrane proteins, type II packing is more common in crystals derived from detergent solution than in crystals derived from LCP.[31]

All three of the new M2-TM variant structures contain well-ordered molecules of racemic *β*-D-octyl-glucoside and *β*-L-octyl-glucoside. The polar headgroup of the detergent molecule interacts with polar side chains of each peptide in a unique manner (Figure 5).

KIH Interactions at the Heterochiral Interface. KIH interactions within antiparallel heterochiral dimers were determined for each structure by quantifying the distance between the side-chain centers-of-mass (COM) of putative pairs of knob and hole residues (Figure 5). Knobs were identified at residues Val28, Ile32, Ile35, Xxx39, and Leu43, where Xxx is either Ile or Ala. This set of residues corresponds to a spacing of 4,3,4,4, which is consistent with a four-residue stutter insertion or a single instance of a hendecad motif (3,4,4).

In a homochiral coiled-coil system a hendecad pattern results in a local unwinding of the corresponding superhelix so that the side chain of the residue in the middle of the 4,4 spacing, i.e., the *h* position, is projected toward the supercoil axis (Figure 3A, green spheres). Based on the 4,3,4,4 spacing assigned to knob residues, Val28 and Xxx42 (Xxx: Ala or Ile) are *h* positions, and the remaining knobs, Ile32, Ile35, and Leu43, are *da* positions. This categorization of knob residues into either *h* or *da* positions lends insight into why a specific heterochiral interface may be preferred.

Residues with smaller side chains such as Ala, Val, or Gly are likely more easily accommodated within *h* positions of parallel, homochiral hendecad motifs compared to residues with bulkier side chains such as Ile. However, this constraint may be relaxed in an antiparallel assembly, as noted by Lupas and Gruber.[9] In line with this steric complementarity hypothesis, we observe that substitution of Ile42 with Ala results in a shift from the offset 3,4-spacing in M2-TM OG to the 3,4,4-spacing observed in the hendecad motif, where Ala is aligned as an *h* position (Figure 6). As an extension of this complementarity hypothesis, we propose that a modification to the interface that increases the size of a particular hole should have a similar effect as decreasing the size of the corresponding knob. Indeed, the M2-TM I42A and I42E structures feature the hendecad motif, which has shifted from the 3,4-M2-TM OG interface so

DOI: 10.1021/jacs.8b11246
J. Am. Chem. Soc. 2019, 141, 1583−1592

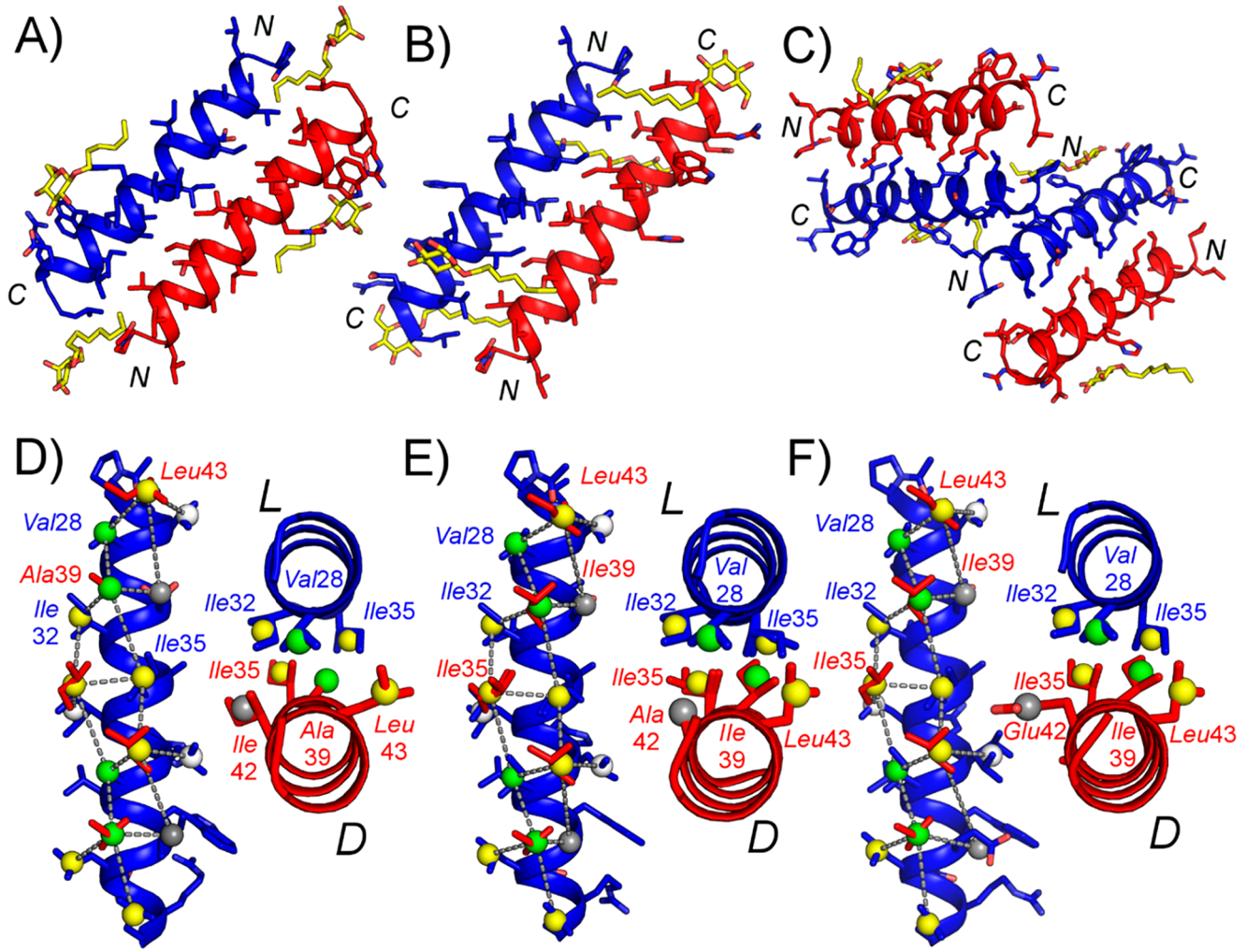

Figure 5. Images highlighting the heterochiral coiled-coil interfaces in each of the three new structures. β-D-octyl-glucoside and β-L-octyl-glucoside molecules are included (yellow sticks). L-Peptide helices are shown in blue and D-peptide helices in red. (A, D) M2-TM I39A; (B, E) M2-TM I42A; (C, F) M2-TM I42E. KIH interactions are indicated in parts D–F by the gray dotted lines; *h* position knobs are shown as green spheres, *ad* position knobs are shown as yellow spheres, modified *k* positions (hole) are shown as gray spheres, and *eg* positions (hole) are shown as white spheres.

that the substituted residue is at the *k* position adjacent to the Ile *h*-position knob (Figure 6).

KTK Interactions at the Heterochiral interface. The structural requirements for formation of an antiparallel dimeric heterochiral coiled-coil assembly include both a nearly straight display of hydrophobic surface area along the side of an α-helix, in the form of a hendecad repeat motif, and sterically compatible KIH interactions of *h* position knobs with holes comprising *k* and *a* positions (Figure 2). However, neither of these requirements necessarily discriminates between a heterochiral and a homochiral association. Therefore, a more detailed description of the geometry underlying each interface is required.

In homochiral coiled-coils, for both parallel and antiparallel assemblies, noncanonical hendecad motifs result in the projection of an *h* position side chain toward the supercoil axis. This projection results in a knob-to-knob (KTK) interaction between *h* position side chains that disrupts canonical KIH packing (Figure 2). Consideration of the angles formed between the C_α–C_β vectors on opposing *h* position residues may in part explain some of the observed preferences for homochiral versus heterochiral and parallel versus antiparallel pairings of helices. Here, we compare heterochiral vs homochiral KTK interactions in the context of antiparallel assemblies and then in the case of parallel assemblies.

In the antiparallel case, the *z*-components of the C_α–C_β vectors on opposing *h* position residues have opposite signs due to the orientations of the backbones (Figure 7A–C). However, the *y*-components of the *h* position C_α–C_β vectors have the same sign for the homochiral case (Figure 7A,B, right panel) but the opposite sign for the heterochiral case (Figure 7C, right panel). Therefore, the angles between opposing C_α–C_β vectors are ~120° for antiparallel homochiral dimers and ~180° for antiparallel heterochiral dimers; the latter values were observed in each of the M2-TM-derived heterochiral dimers. From a purely steric perspective, the heterochiral dimer seems more favorable than the homochiral dimer; however, the fact that side chains are oriented in completely opposite directions precludes any other type of interaction between side chains, such as salt-bridging, cation-π pairing, or hydrogen-bonding interactions.

In the parallel case, the *z*-components of the *h* position C_α–C_β vectors have the same sign for heterochiral and homochiral dimers (Figure 7D, left panel).

DOI: 10.1021/jacs.8b11246
J. Am. Chem. Soc. 2019, 141, 1583–1592

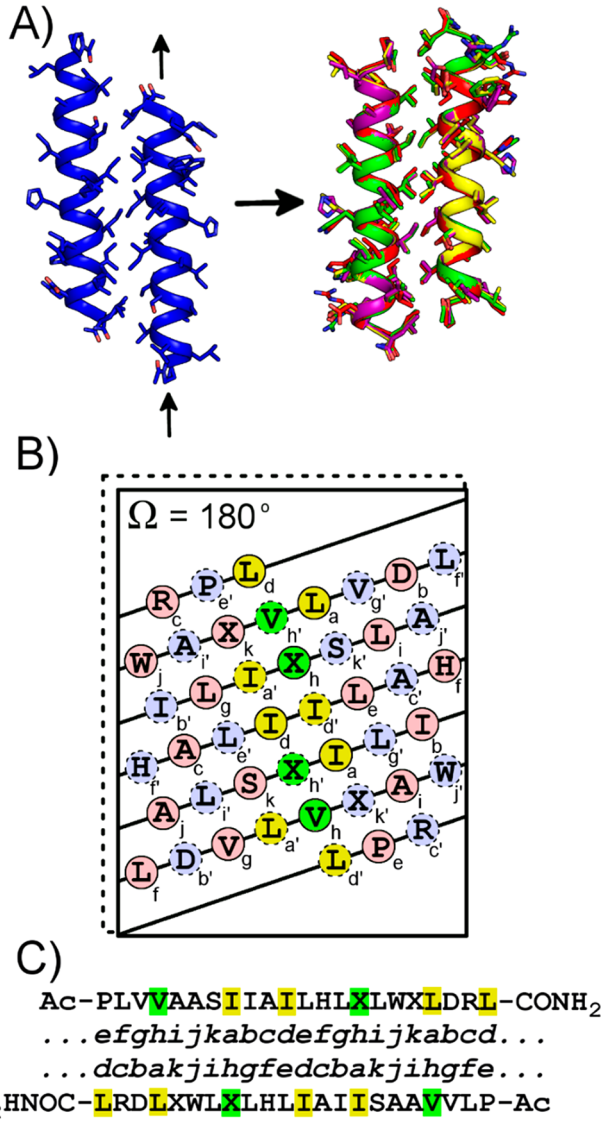

Figure 6. Comparisons of L-peptide/D-peptide juxtapositions among different heterochiral coiled-coil structures crystallized from racemic *β*-octyl-glucoside solution. (A) M2-TM OG dimer, with a heptad repeat, is shown in blue. The three new variants, with hendacad repeats, are overlaid (I39A, red; I42A, green; I42E1, yellow; I42E2, purple). (B) Helical net diagram for the antiparallel hendecad interface (180° crossing angle) shows that substituted residues become aligned at the *h* (knob) and *g* (hole) positions. Substitution positions (demarcated by X), *ad* positions (yellow circles) and *h* positions (green circles) correspond to a (C) sequence alignment of M2-TM with a hendecad registry.

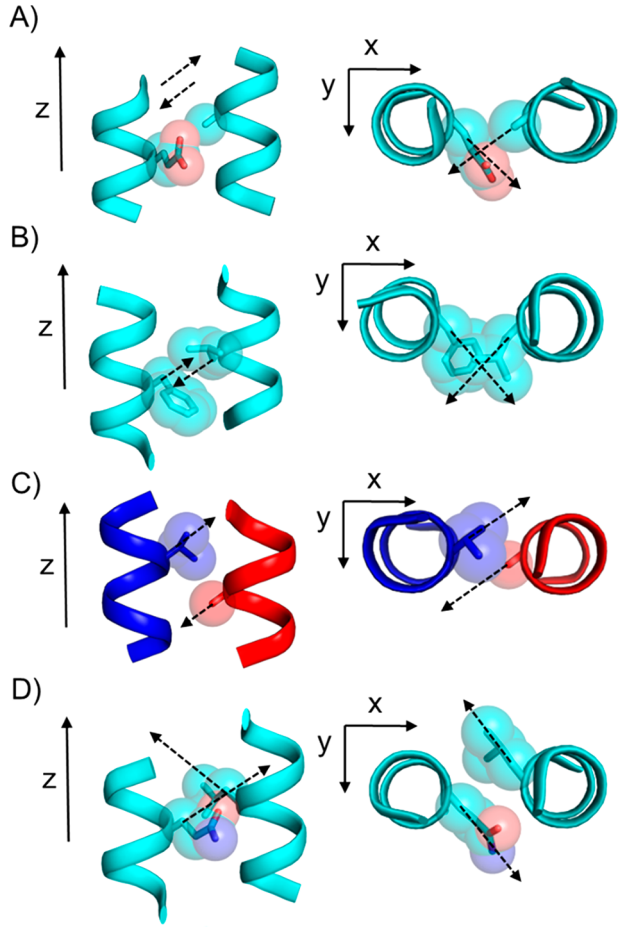

Figure 7. Longitudinal and axial views of dimeric KTK interactions at hendecad *h* positions shown for different types of coiled-coil dimer. (A) Antiparallel, homochiral dimer (PDB: 4LTB, Glu267 to Ala234). (B) Antiparallel, homochiral dimer (PDB: 3VEM, Phe1776 to Leu1765). (C) Antiparallel heterochiral dimer (M2-TM I39A; L-peptide in blue; D-peptide in red, Val28 to Ala39). (D) Parallel, homochiral dimer (PDB: 4HH3, Gln134 to Leu130). In each case, the Cartesian coordinate directions discussed in the text are shown in addition to the C_α–C_β vectors (dashed arrows).

Although no atomic-resolution structure is currently available for the parallel heterochiral case, presumably the orientation of the C_α–C_β vector *z*-component would be unaffected by inversion of stereochemistry. However, for a parallel dimer, the *y*-components of the C_α–C_β vectors are of opposite sign for the homochiral case and of the same sign for the hypothetical heterochiral case (Figure 7D). Thus, from a purely steric perspective, there is maximum repulsion for the heterochiral case but less steric overlap for the homochiral case. The parallel, homochiral *h* position residues should have less steric repulsion than those of the antiparallel homochiral case. Based on this simple C_α–C_β vector analysis, an antiparallel heterochiral coiled coil (Figure 7C) is the only pairing combination that completely mitigates sterically unfavorable KTK interactions in the presence of 3,4,4-spacing.

Parameterization of a Heterochiral Helical Assembly. We developed a parametrization of heterochiral coiled-coil assemblies that we employed to compare structural features among heterochiral coiled-coil M2-TM variants. These parametric models were then fitted to C_α atom coordinates from each racemic M2-TM crystal structure (Table 1). Pertinent model parameters include a value to quantify the tightness of packing among interfaces to test our steric complementarity hypothesis, in addition to a helical frequency parameter to test for the presence of a hendecad motif. In general, the parametrization of folded protein structures and assemblies is useful for *de novo* design purposes.[17,33] Mapping these complex structures to an *N*-dimensional model, where *N* is relatively small compared to the number of atoms in the structure, allows for efficient grid searching of the available structural space. Several homochiral coiled-coil design strategies have employed the Crick coiled-coil parametric equations to generate backbone conformations that can sample available structural space at a modest computational cost.[17−19,33] The Crick

DOI: 10.1021/jacs.8b11246
J. Am. Chem. Soc. 2019, 141, 1583−1592

Table 1. Parameterized Heterochiral Coiled-Coil Model Values Derived from Racemic M2-TM Crystal Structures

variant	PDB	R_0 (Å)	R_1 (Å)	ω_1 (deg/res)	φ^a (deg)	d (Å/res)	Δz (Å)	ΔZ_{off} (Å)	RMSD (Å)
I39A	6MPL	4.74	2.31	98.2	143.0	1.50	3.34	2.16	0.19
I42A	6MPM	4.90	2.30	98.7	142.1	1.50	3.98	1.48	0.28
I42E1	6MPN	5.04	2.28	100.1	128.7	1.50	3.93	1.47	0.33
I42E2	6MPN	5.00	2.29	99.3	138.4	1.50	3.95	1.49	0.32
M2LCP1	4RWB	5.01	2.29	98.6	143.1	1.50	3.96	1.50	0.17
M2LCP2	4RWB	5.06	2.31	98.2	147.1	1.49	4.06	1.41	0.22
M2OG	4RWC	5.14	2.30	98.1	162.0	1.50	−6.26	0.77	0.23

[a]The parameter φ quantifies a phase shift with respect to the superhelical axis for individual helices. In the racemic M2-TM system, there are two φ values that are related by inversion symmetry. The φ value for the right-handed helix is listed here.

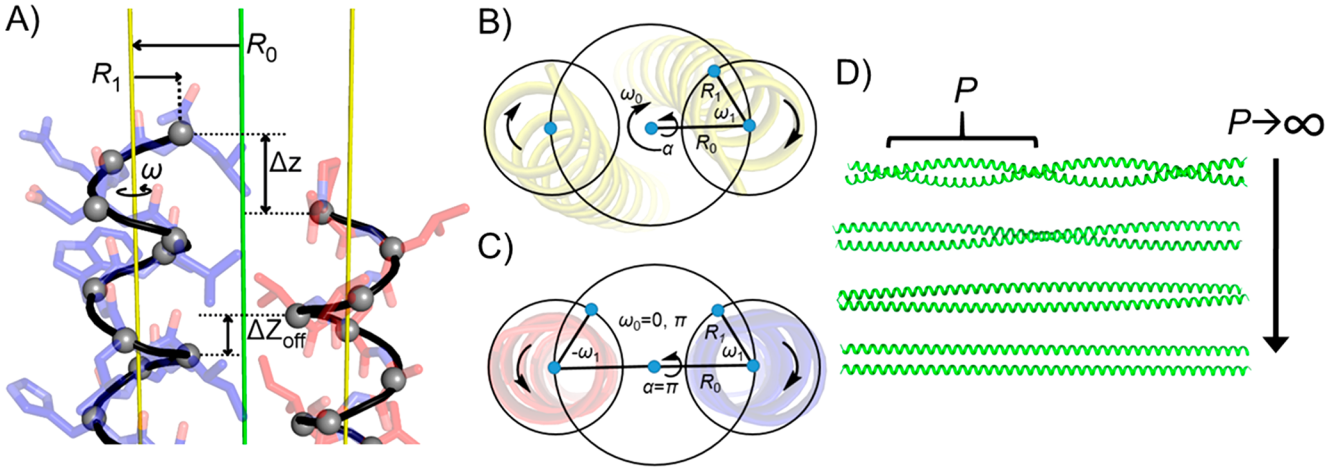

Figure 8. Parametrized model for a heterochiral coiled-coil. (A) Model illustrated for M2-TM I42A. R_0 is the radius of the superhelix, centered on the green axis, and R_1 is the radius of an individual helix, centered on the yellow axis. The model assumes no supercoiling, so that the yellow axes are at phases of 0 and 180° with respect to the green axis and correspond to each individual helical axis. The parametric curves (black) trace through the Cα atoms (gray spheres), and the helicity depends only on the helical frequency of each helix, ω_1, and the handedness of the helix; Δz is an offset term that allows for translational motion parallel to the superhelical axis (green). ΔZ_{off} describes the closest offset distance between portions of the parametric curves that are in phase. ΔZ_{off} by definition is constrained to less than 2.7 Å for a hendecad. (B) Conventional Crick coiled-coil parameters shown for an axial view of a homochiral coiled-coil dimer (GCN4; PDB 2ZTA). (C) Crick coiled-coil parameters shown for an axial view of a heterochiral coiled-coil dimer (M2-TM I42A). (D) As the pitch, P, of a coiled-coil super helix becomes larger, the angular frequency of the superhelix goes to zero (as $P \rightarrow \infty$, $\omega_0 \rightarrow 0$; helices of increasing pitch length were generated with CCBuilder[23]).

equations implicitly describe parallel homochiral assemblies, although as originally described these equations are concerned solely with the arrangement of backbone atoms and are therefore equally suited for parallel or antiparallel assemblies. In an effort to more accurately describe antiparallel assemblies, recent adaptations of the Crick equations have included a translational offset term, as defined by Grigoryan and DeGrado.[17,33] With a few assumptions, these equations can be adapted to describe an antiparallel, heterochiral dimer.

The Crick parametric equations for a coiled coil are based on the principle of supercoiling, which causes multiple α-helices to twist around a superhelical axis. This supercoiling is defined by an angular frequency, ω_0, which depends on the pitch of the supercoil, P (the unit distance periodicity). A position, such as that of a backbone atom, on one of the n helices (n = 2 in Figure 8A−C) can be determined if the initial phase of a helix, φ_i, and the helical frequency, ω_1, are known. To determine pertinent model parameters and to compare parameters between M2-TM structures, we modified the Crick equations for the case of a heterochiral coiled-coil dimer so that the parameters include R_0, the radius of the coiled-coil, R_1, the radius of an individual α-helix, ω, the frequency of each α-helix, φ, the initial phase of each α-helix, d, the rise/residue of each α-helix, and Δz, the offset between α-helices (Figure 8A).

In a heterochiral coiled-coil system, a major difference from the original Crick equations is that there is no supercoiling due to the required maintenance of a 180° crossing angle. Therefore, the z-coordinate is set based on the rise per residue of an individual α-helix. The superhelix is simply two parallel lines that have phases of 0 or π radians. Another departure from the Crick system is the inversion of the sign of the helical phase due to the presence of a left-handed α-helix. We adopted the Δz and ΔZ_{off} terms described by Grigoryan and DeGrado,[33] where the sign of Δz depends on the direction the left-handed helix shifts with respect to the right-handed helix; a shift in the C → N direction results in a positive value.[33] ΔZ_{off} is defined as the absolute value of the minimum distance between z values on the parametric helical curves that have a phase of 180°, i.e., the minimal distance (z direction) between points along the curve that point inward toward the central "superhelical" axis (Figure 6B). Our system is further simplified by the crystallographic inversion center in the middle of the coiled-coil interface, which constrains the helical radius, R_1, and helical frequency, ω, to singular values for the two-helix system. The RMSD between the parametric helical curves and the atomic coordinates of the C_α-atoms was used as the objective function during nonlinear regression to determine the parametric model parameters for each

DOI: 10.1021/jacs.8b11246
J. Am. Chem. Soc. 2019, 141, 1583−1592

heterochiral M2-TM structure (Table 1; fitting procedure described in Supporting Information).

The value for R_0 quantifies the tightness of packing between two helices. More closely packed helices will have a smaller R_0 value, which ranges from 4.74 Å (M2-TM I39A) to 5.14 Å (M2-TM OG). This difference is consistent with our rationale for the observed shift from a 3,4-spacing in the M2-TM OG structure to a 3,4,4 hendecad in the M2-TM I39A structure, in which the Ile → Ala substitution at the *h* position is correlated with a more closely packed interface. The M2-TM I42A R_0 value of 4.90 Å falls between the range bounded by M2-TM I39A (4.74 Å) and M2-TM OG (5.14 Å). This observation suggests that a smaller *h* position knob, as in M2-TM I39A, is more beneficial in terms of close packing than is a smaller hole, as in M2-TM I42A. Close packing at interfaces involving Ala residues has been documented in the Alacoil motif found in globular proteins, in which alanine side chains are projected into the upper or lower triad of residues that form the corresponding hole.[34] This arrangement results in extremely small R_0 values (<4.5 Å).[34] The two M2-TM I42E R_0 values, 5.00 and 5.04 Å, are smaller than that of M2-TM OG (5.14 Å), but are similar to the values of 5.01 and 5.06 Å in M2-TM LCP (PDB: 4RWB), which contains Ile at both the *h* position knob and the *k* position hole. For a point of reference, the distribution median of R_0 was reported to be 4.82 Å for antiparallel, homochiral coiled-coil dimers in the CC+ database.[33,35]

Finally, the helical frequencies observed for M2-TM I39A (98.2°/res), I42A (98.7°/res), and one of the I42E dimers (99.3°/res) are consistent with the hendecad hypothesis, which predicts a frequency of 98.2°/res. The second M2-I42E dimer frequency (100.1°/res) has the largest deviation from the predicted value; however, the margin of difference is less than the margin between the I42E frequency and a heptad frequency (102.9°/res, for two 360° turns over seven residues). The previously reported M2-TM OG and LCP structures[21] also have frequencies consistent with a hendecad repeat.

Other Motifs Compatible with Heterochiral Coiled-Coils. The main feature of a hendecad motif that makes it compatible with an antiparallel, heterochiral coiled-coil is the marginal difference between the residue frequency of the motif (3.67 residues/turn) and the geometry of an ideal α-helix (3.65 residues/turn). The distortion of the α-helix required to accommodate the hendecad motif is less than the distortion required to accommodate the heptad motif (3.50 residues/turn); therefore, helices can readily adopt a conformation that results in a near-linear display of hydrophobic side chains. These concepts suggest other possible combinations of three and four residue spacings that can achieve a linear side chain array. For example, an 18-residue spacing over five turns requires a periodicity of approximately 100°/residue or 3.60 residues/turn. Recent *de novo* computational efforts have exploited this 18-residue motif for the design of homochiral coiled-coils.[16] Motifs that result in minimal supercoiling, or constrained models in general, may be tractable from a design standpoint in part due to a decreased search space compared to coiled-coil systems that display supercoiling.[18,33]

In 1953, Crick recognized that dimeric heterochiral coiled-coils would necessarily have 0° or 180° crossing angles akin to helical gears of opposite sense.[13] Each of the aforementioned motifs (hendecad and 18-residue) is predicated on a homodimeric interaction. There is a third possibility for a heterochiral interaction if different sequences are considered, i.e., the dimeric pair is not enantiomorphic. In such cases, the L- and D-peptides could feature different sequence repeat patterns. In a system comprising entirely L-amino acids, for example, if the periodicity of an ideal α-helix is considered as a "baseline", then the "drift" of a heptad motif (3.50 residues/turn) with respect to the baseline is left-handed and approximately −0.15 residues/turn. A 15-residue, pentadecad, motif over four turns has a periodicity of 3.75 residues/turn and, thus, a right-handed drift of approximately +0.10 residues/turn with respect to the baseline. Inversion of the chirality of a pentadecad helix, via use of D-residues, will invert the handedness of the hydrophobic side chain display so that it is now left-handed and commensurate with the side chain display from an L-peptide α-helix with a heptad repeat. Following this simple model, other heterodimeric, heterochiral pairings are possible, such as an L-peptide hendecad motif paired with a D-peptide 18-residue motif (or vice versa).

CONCLUSIONS

The three new crystal structures described here expand our understanding of the factors that influence the formation of heterochiral antiparallel coiled-coil dimers. Analysis of these structures, along with two previously reported examples, supports the hypothesis that antiparallel coiled-coil association of α-helices with opposite handedness (as generated by L- vs D-amino acid residues) is most compatible with an 11-residue sequence repeat (hendecad), in contrast to the 7-residue sequence repeat (heptad) that is most common among coiled-coils formed from α-helices with the same handedness. In the heptad pattern, hydrophobic residues at residues *i*, *i*+3, *i*+7, *i*+10, *i*+14, etc. (3,4 spacing) align to form a stripe along one side of each helix, and burial of hydrophobic stripes against one another drive coiled-coil association. In the hendecad pattern, hydrophobic residues at residues *i*, *i*+3, *i*+7, *i*+11, *i*+14, *i*+18, *i*+22, etc. (3,4,4 spacing) form the stripe. Because of the interplay between geometric periodicity of the α-helical conformation and sequence periodicity, these different arrangements of hydrophobic residues influence quaternary structural preferences. The data reported here, along with a parametrization of heterochiral α-helix assemblies, should be useful for efforts to design D-peptides that bind to specific L-peptide partners.

PARAMETRIC EQUATIONS

The Crick equations for a canonical coiled-coil have the general form

$$x = R_0 \cos \omega_0 - R_1 \cos \omega_0 \sin \varphi + R_1 \cos \alpha \sin \omega_0 \sin \varphi$$

$$y = R_0 \sin \omega_0 - R_1 \sin \omega_0 \cos \varphi - R_1 \cos \alpha \cos \omega_0 \sin \varphi$$

$$z = P(\omega/2\pi) + R_1 \sin \alpha \sin \varphi$$

$$x_i = R_0 \cos(2\pi z/P + \tau_i) + x \cos(2\pi z/P + \tau_i)$$

$$-y \cos \alpha \sin(2\pi z/P + \tau_i)$$

$$y_i = R_0 \sin(2\pi z/P + \tau_i) + x \sin(2\pi z/P + \tau_i)$$

$$-y \cos \alpha \cos(2\pi z/P + \tau_i)$$

$$z_i = z - y \sin \alpha$$

$$\tau_i = 2\pi(i - 1)/n$$

DOI: 10.1021/jacs.8b11246
J. Am. Chem. Soc. 2019, 141, 1583−1592

where P is the pitch of the superhelix; x, y, and z define points along the superhelix; α is the pitch angle; and x_i, y_i, and z_i define points along the n-th helix (Figure 8B).

The parametric equations for a heterochiral coiled-coil dimer are therefore

$$x_r = R_0 + R_1 \cos(\omega t + \varphi_r)$$

$$y_r = R_1 \sin(\omega t + \varphi_r)$$

$$z_r = dt + \Delta z$$

$$x_l = -R_0 - R_1 \cos(-\omega t + \varphi_l)$$

$$y_l = R_1 \sin(-\omega t + \varphi_l)$$

$$z_l = dt$$

where t is the residue index (t = 1, 2, ..., 22 for the M2-TM variants), and the subscript r or l denotes a right or left-handed helix, respectively.

■ ASSOCIATED CONTENT

Supporting Information

The Supporting Information is available free of charge on the ACS Publications website at DOI: 10.1021/jacs.8b11246.

Experimental details regarding peptide synthesis and characterization; X-ray structure solution and refinement; (PDF)

Parametric model fitting data (XLSX)

■ AUTHOR INFORMATION

Corresponding Authors

*forest@bact.wisc.edu

*gellman@chem.wisc.edu

ORCID

Dale F. Kreitler: 0000-0003-4758-7913

Samuel H. Gellman: 0000-0001-5617-0058

Present Addresses

#(D.F.K.) Department of Structural Biology, University at Buffalo, Buffalo, NY 14203.

∇(D.E.M.) Gilead Sciences, Inc., Foster City, CA 94404.

Notes

The authors declare no competing financial interest.

■ ACKNOWLEDGMENTS

This work was supported in part by the NIH (R01GM061238 to S.H.G.). D.F.K. was supported in part by a Biotechnology Training Grant (T32 GM00839). This research used resources of the Advanced Photon Source, a U.S. Department of Energy (DOE) Office of Science User Facility operated for the DOE Office of Science by Argonne National Laboratory, under Contract No. DE-AC02-06CH11357. Use of the LS-CAT Sector 21 was supported by the Michigan Economic Development Corporation and the Michigan Technology Tri-Corridor (Grant 085P1000817).

■ REFERENCES

(1) Welch, B. D.; VanDemark, A. P.; Heroux, A.; Hill, C. P.; Kay, M. S. Potent D-Peptide Inhibitors of HIV-1 Entry. *Proc. Natl. Acad. Sci. U. S. A.* **2007**, *104* (43), 16828−16833.

(2) Liu, M.; Li, C.; Pazgier, M.; Li, C.; Mao, Y.; Lv, Y.; Gu, B.; Wei, G.; Yuan, W.; Zhan, C.; Lu, W.-Y.; Lu, W. D-Peptide Inhibitors of the p53-MDM2 Interaction for Targeted Molecular Therapy of Malignant Neoplasms. *Proc. Natl. Acad. Sci. U. S. A.* **2010**, *107* (32), 14321−14326.

(3) Van Groen, T.; Wiesehan, K.; Funke, S. A.; Kadish, I.; Nagel-Steger, L.; Willbold, D. Reduction of Alzheimer's Disease Amyloid Plaque Load in Transgenic Mice by D3, a D-Enantiomeric Peptide Identified by Mirror Image Phage Display. *ChemMedChem* **2008**, *3* (12), 1848−1852.

(4) Schumacher, T. N. M.; Mayr, L. M.; Minor, D. L., Jr.; Milhollen, M. A.; Burgess, M. W.; Kim, P. S. Identification of D-Peptide Ligands Through Mirror-Image Phage Display. *Science* **1996**, *271*, 1854−1857.

(5) Chang, H. N.; Liu, B. Y.; Qi, Y. K.; Zhou, Y.; Chen, Y. P.; Pan, K. M.; Li, W. W.; Zhou, X. M.; Ma, W. W.; Fu, C. Y.; Qi, Y. M.; Liu, L.; Gao, Y. F. Blocking of the PD-1/PD-L1 Interaction by a D-Peptide Antagonist for Cancer Immunotherapy. *Angew. Chem., Int. Ed.* **2015**, *54* (40), 11760−11764.

(6) Mandal, K.; Uppalapati, M.; Ault-Riché, D.; Kenney, J.; Lowitz, J.; Sidhu, S. S.; Kent, S. B. H. Chemical Synthesis and X-Ray Structure of a Heterochiral {D-Protein Antagonist plus Vascular Endothelial Growth Factor} Protein Complex by Racemic Crystallography. *Proc. Natl. Acad. Sci. U. S. A.* **2012**, *109* (37), 14779−14784.

(7) Guichard, G.; Benkirane, N.; Zeder-Lutz, G.; van Regenmortel, M. H. V.; Briand, J.-P.; Muller, S. Antigenic Mimicry of Natural L-Peptides with Retro-Inverso-Peptidomimetics. *Proc. Natl. Acad. Sci. U. S. A.* **1994**, *91* (21), 9765−9769.

(8) Li, C.; Pazgier, M.; Li, J.; Li, C.; Liu, M.; Zou, G.; Li, Z.; Chen, J.; Tarasov, S. G.; Lu, W. Y.; Lu, W. Limitations of Peptide Retro-Inverso Isomerization in Molecular Mimicry. *J. Biol. Chem.* **2010**, *285* (25), 19572−19581.

(9) Lupas, A. N.; Gruber, M. The Structure of α-Helical Coiled Coils. *Adv. Protein Chem.* **2005**, *70*, 37−38.

(10) Woolfson, D. N. The Design of Coiled-Coil Structures and Assemblies. *Adv. Protein Chem.* **2005**, *70*, 79−112.

(11) Hicks, M. R.; Walshaw, J.; Woolfson, D. N. Investigating the Tolerance of Coiled-Coil Peptides to Nonheptad Sequence Inserts. *J. Struct. Biol.* **2002**, *137*, 73−81.

(12) Moutevelis, E.; Woolfson, D. N. A Periodic Table of Coiled-Coil Protein Structures. *J. Mol. Biol.* **2009**, *385* (3), 726−732.

(13) Crick, F. H. C. The Packing of α-Helices: Simple Coiled-Coils. *Acta Crystallogr.* **1953**, *6* (8), 689−697.

(14) Crick, F. H. C. Is a-Keratin a Coiled Coil. *Nature* **1952**, *170*, 882−883.

(15) Crick, F. H. C. The Fourier Transform of a Coiled-Coil. *Acta Crystallogr.* **1953**, *6* (8), 685−689.

(16) Bhardwaj, G.; Mulligan, V. K.; Bahl, C. D.; Gilmore, J. M.; Harvey, P. J.; Cheneval, O.; Buchko, G. W.; Pulavarti, S. V. S. R. K.; Kaas, Q.; Eletsky, A.; Huang, P.-S.; Johnsen, W. A.; Greisen, P. J.; Rocklin, G. J.; Song, Y.; Linsky, T. W.; Watkins, A.; Rettie, S. A.; Xu, X.; Carter, L. P.; Bonneau, R.; Olson, J. M.; Coutsias, E.; Correnti, C. E.; Szyperski, T.; Craik, D. J.; Baker, D. Accurate de Novo Design of Hyperstable Constrained Peptides. *Nature* **2016**, *538* (7625), 329−335.

(17) Huang, P.-S.; Oberdorfer, G.; Xu, C.; Pei, X. Y.; Nannenga, B. L.; Rogers, J. M.; DiMaio, F.; Gonen, T.; Luisi, B.; Baker, D. High Thermodynamic Stability of Parametrically Designed Helical Bundles. *Science* **2014**, *346* (6208), 481−485.

(18) Joh, N. H.; Wang, T.; Bhate, M. P.; Acharya, R.; Wu, Y.; Grabe, M.; Hong, M.; Grigoryan, G.; DeGrado, W. F. *De Novo Design of a Transmembrane Zn^{2+}-Transporting Four-Helix Bundle. Science* **2014**, *346* (6216), 1520−1524.

(19) Thomson, A. R.; Wood, C. W.; Burton, A. J.; Bartlett, G. J.; Sessions, R. B.; Brady, R. L.; Woolfson, D. N. Computational Design of Water-Soluble Alpha-Helical Barrels. *Science* **2014**, *346* (6208), 485−488.

(20) Pauling, L.; Corey, R. B. Two Rippled-Sheet Configurations of Polypeptide Chains, and a Note about the Pleated Sheets. *Proc. Natl. Acad. Sci. U. S. A.* **1953**, *39*, 253−256.

(21) Mortenson, D. E.; Steinkruger, J. D.; Kreitler, D. F.; Perroni, D. V.; Sorenson, G. P.; Huang, L.; Travis, B. R.; Mahanthappa, M. K.;

Forest, K. T.; Gellman, S. H. High-Resolution Structures of a Heterochiral Coiled Coil. *Proc. Natl. Acad. Sci. U. S. A.* **2015**, *112* (43), 13144−13149.
(22) Acharya, R.; Carnevale, V.; Fiorin, G.; Levine, B. G.; Polishchuk, A. L.; Balannik, V.; Samish, I.; Lamb, R. A.; Pinto, L. H.; DeGrado, W. F.; Klein, M. L. Structure and Mechanism of Proton Transport through the Transmembrane Tetrameric M2 Protein Bundle of the Influenza A Virus. *Proc. Natl. Acad. Sci. U. S. A.* **2010**, *107* (34), 15075−15080.
(23) Wood, C. W.; Bruning, M.; Ibarra, A. A.; Bartlett, G. J.; Thomson, A. R.; Sessions, R. B.; Brady, R. L.; Woolfson, D. N. CCBuilder: An Interactive Web-Based Tool for Building, Designing and Assessing Coiled-Coil Protein Assemblies. *Bioinformatics* **2014**, *30* (21), 3029−3035.
(24) Sia, S. K.; Kim, P. S. A Designed Protein with Packing between Left-Handed and Right-Handed Helices. *Biochemistry* **2001**, *40* (30), 8981−8989.
(25) Harbury, P. B.; Plecs, J. J.; Tidor, B.; Alber, T.; Kim, P. S. High-Resolution Protein Design with Backbone Freedom. *Science* **1998**, *282* (5393), 1462−1467.
(26) Peters, J.; Nitsch, M.; Kühlmorgen, B.; Golbik, R.; Lupas, A.; Kellermann, J.; Engelhardt, H.; Pfander, J. P.; Müller, S.; Goldie, K.; Engel, A.; Stetter, K. O.; Baumeister, W. Tetrabrachion: A Filamentous Archaebacterial Surface Protein Assembly of Unusual Structure and Extreme Stability. *J. Mol. Biol.* **1995**, *245* (4), 385−401.
(27) Brown, J. H.; Cohen, C.; Parry, D. A. D. Heptad Breaks in Alpha-Helical Coiled Coils: Stutters and Stammers. *Proteins: Struct., Funct., Genet.* **1996**, *26* (2), 134−145.
(28) Lupas, A.; Müller, S.; Goldie, K.; Engel, A. M.; Engel, A.; Baumeister, W. Model Structure of the Omp Alpha Rod, a Parallel Four-Stranded Coiled Coil from the Hyperthermophilic Eubacterium Thermotoga Maritima. *J. Mol. Biol.* **1995**, *248* (1), 180−189.
(29) Weis, W. I.; Brünger, A. T.; Skehel, J. J.; Wiley, D. C. Refinement of the Influenza Virus Hemagglutinin by Simulated Annealing. *J. Mol. Biol.* **1990**, *212* (4), 737−761.
(30) Hicks, M. R.; Holberton, D. V.; Kowalczyk, C.; Woolfson, D. N. Coiled-Coil Assembly by Peptides with Non-Heptad Sequence Motifs. *Folding Des.* **1997**, *2* (3), 149−158.
(31) Ostermeier, C.; Michel, H. Crystallization of Membrane Proteins. *Curr. Opin. Struct. Biol.* **1997**, *7*, 697−701.
(32) Cherezov, V. Lipidic Cubic Phase Technologies for Membrane Protein Structural Studies. *Curr. Opin. Struct. Biol.* **2011**, *21* (4), 559−566.
(33) Grigoryan, G.; DeGrado, W. F. Probing Designability via a Generalized Model of Helical Bundle Geometry. *J. Mol. Biol.* **2011**, *405* (4), 1079−1100.
(34) Gernert, K. M.; Surles, M. C.; Labean, T. H.; Richardson, J. S.; Richardson, D. C. The Alacoil: A Very Tight, Antiparallel Coiled-Coil of Helices. *Protein Sci.* **1995**, *4* (11), 2252−2260.
(35) Testa, O. D.; Moutevelis, E.; Woolfson, D. N. CC+: A Relational Database of Coiled-Coil Structures. *Nucleic Acids Res.* **2009**, *37*, 315−322.

DOI: 10.1021/jacs.8b11246
J. Am. Chem. Soc. 2019, 141, 1583−1592